Engineering the Temporal Response of Photoconductive Photodetectors via Selective Introduction of Surface Trap States

Gerasimos Konstantatos, Larissa Levina, Armin Fischer, and Edward H. Sargent*

Department of Electrical and Computer Engineering, University of Toronto, 10 King's College Road, Toronto ON M5S 3G4, Canada

ABSTRACT

Photoconductive photodetectors fabricated using simple solution-processing have recently been shown to exhibit high gains (>1000) and outstanding sensitivities ($D^* > 10^{13}$ Jones). One ostensible disadvantage of exploiting photoconductive gain is that the temporal response is limited by the release of carriers from trap states. Here we show that it is possible to introduce specific chemical species onto the surfaces of colloidal quantum dots to produce only a single, desired trap state having a carefully selected lifetime. In this way we demonstrate a device that exhibits an attractive photoconductive gain (>10) combined with a response time (~25 ms) useful in imaging. We achieve this by preserving a single surface species, lead sulfite, while eliminating lead sulfate and lead carboxylate. In doing so we preserve the outstanding sensitivity of these devices, achieving a specific detectivity of 10^{12} Jones in the visible, while generating a temporal response suited to imaging applications.

Optical sensing in visible and near-infrared regions is of utmost importance for conventional imaging,[1] passive night vision,[2] and biomedical imaging.[3] The sensitivity of a photodetecting material is quantified through the figure of merit D^*, the specific detectivity, in units of Jones. A high D^* value corresponds to a device having, for its area and detection bandwidth, a high ratio of signal-to-noise for a given light level.

Also important in photodetection is temporal response. If the response of a photodetector to an optical transient exceeds the frame period, then lag, or ghosting, will be perceptible in the image. Conventional imaging applications typically require frame rates in the range of 10, 15, 30, or 60 frames s^{-1}. Temporal responses having time constants in the range of tens of milliseconds are thus required.

There exists a high degree of interest in novel materials, and novel processing methods, for the realization of innovative imaging systems. Solution-processed optoelectronic materials offer large area at low cost,[4] the benefits of physical flexibility, the 100% fill factor associated with a top-surface photodetector technology,[5] and the capacity to sense wavelengths, such as those in the short-wavelength IR,[6] not accessible to conventional electronic materials such as silicon.

A novel approach, based on colloidal quantum dots,[5–8] has recently emerged that addresses the limitations of conventional bulk semiconductor technology. However, to date,

colloidal quantum dot photodetectors have exhibited either superb sensitivities ($D^* > 10^{13}$ Jones) but slow response (hundreds of millisecond transients)[5,6] or rapid response (megahertz and above) but low sensitivity ($D^* < 10^{10}$ Jones),[8] but not both requisite features simultaneously.

Here we show that it is possible, through careful control over materials composition, to engineer the temporal response of photoconductive photodetectors to achieve outstanding sensitivity and acceptable temporal response simultaneously.

Photoconductive gain is given by τ_c/τ_t, where τ_t is the time for the flowing carrier to transit the extent of the device and τ_c is the carrier lifetime. From a sensitivity point of view alone, this argues for longer trap state lifetimes. However, the temporal response is directly determined by the carrier lifetime. The challenge of practical photoconductive photodetector design is thus to establish a suitable balance between gain and temporal response and to control material composition with care to implement the resultant design.

We previously investigated the energy levels associated with trap states in PbS colloidal quantum dot photodetectors[9] that exhibit gains on the order of a hundred A/W. Three sensitizing centers, the energy levels of which resided approximately 0.1, 0.2, and 0.34 eV from the conduction band, resulted in carrier lifetimes of ~60, 300, and 2000 ms (Figure 1). Though the shortest lifetime of 30 ms is suited for many imaging applications, the longer ones, which
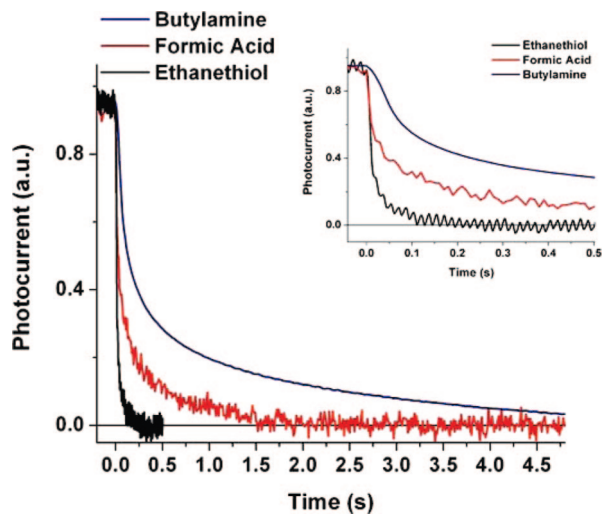
Figure 1. Temporal response of photocurrent in butylamine, formic acid, and ethanethiol treated nanocrystal films. Butylamine treated films exhibit a photocurrent decay with multiple time constants of approximately 60, 300, and 2000 ms. Formic acid treated devices yield a main photocurrent decay time constant of ~420 ms. Ethanethiol treated devices show a faster photocurrent decay with a time constant of ~27 ms, the photocurrent decays to the dark current state within less than 200 ms (shown in the inset).

dominate at lower optical intensities in view of their lower energies, introduce unacceptable lag.

Herein we present a framework that allows identifying specific oxide species existent on the quantum dots surface as sensitizing centers and their mapping to their corresponding time constants. We elucidate a device fabrication sequence that facilitates suppression of the longest lived trap states, preserving sensitization only via the shortest (temporally), thus the shallowest (energetically), trap state.

Photoconductive devices were fabricated by spin coating oleic acid-capped nanocrystals[10] onto prepatterned interdigitated gold electrodes. The quantum dots' first excitonic peak lays at 790 nm. The thickness of the devices was kept constant around 250 nm. The active area of the device is circumscribed by the 5 μm separation of the electrodes and their 3 mm length. For illumination, a 642 nm light-emitting diode producing optical intensity at the sample of 3.1 μW/cm^2 was used unless otherwise stated. The bias applied to the devices studied herein was 10 V, corresponding to an electric field of 2 V/μm. All photoconductive measurements[11] were performed with devices loaded in a cryostat under vacuum conditions so that oxygen and moisture chemadsorption effects are eliminated.

X-ray photoelectron spectroscopy (XPS) analysis of nanocrystals treated using butylamine revealed the presence of lead sulfate ($PbSO_4$), lead sulfite ($PbSO_3$), and lead carboxylate attributable to oleic acid ligands attached to the nanoparticles' surfaces. XPS analysis of the S 2p signal yields a peak at 165.5 eV attributable to $PbSO_3$ and a peak 167.8 eV resulting from $PbSO_4$ (Figure 2b), whereas Pb 4f signal analysis revealed oxidized states assigned to $PbSO_4$ and $PbSO_3$ at 138.5 eV and a highly oxidized state of Pb found at 139.1 eV associated with Pb−carboxylate (Figure 2a). To verify this last finding, we carried out XPS on Pb−oleate
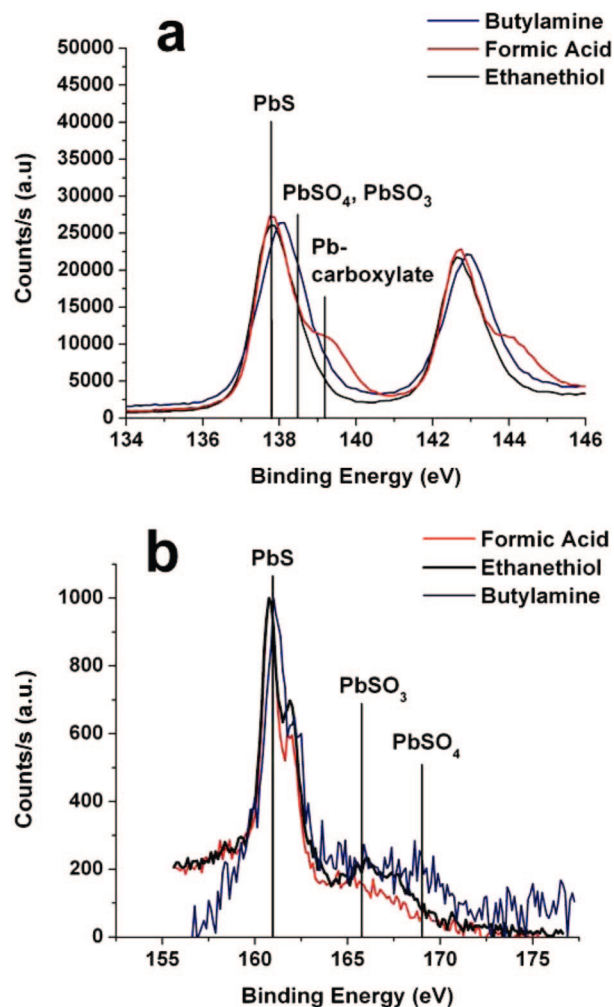

Figure 2. XPS spectra of Pb 4f (a) and S 2p (b) signal from butylamine, formic acid, and ethanethiol treated nanocrystal films used as photodetectors. The lines show the energy levels associated with the reported species.

(the same used for PbS nanocrystal synthesis), revealing a single peak of Pb at 139.1 eV (see Supporting Information for detailed analysis of XPS results).

We then investigated whether we could correlate the lead carboxylate peak (due to the oleic acid−Pb bond) with a corresponding sensitizing trap state having a specific temporal response. We treated nanocrystal films with a 30% by volume solution of formic acid in acetonitirile to exchange the long oleic acid ligand with a shorter one. In so doing we reduced inter-nanoparticle spacing while preserving the carboxylate moiety bound to Pb atoms on the nanocrystal surface. In this way, we transformed insulating devices into photoconductive detectors. Temporal measurements of photocurrent response revealed a main time constant of ~420 ms (Figure 1) and also a faster component with time constant ~33 ms. XPS revealed an oxidized component to the Pb 4f signal at 139.1 eV characteristic of the Pb−carboxylate group, as illustrated in Figure 2a as well as a signal at 138.5 eV arising from the existence of $PbSO_3$ as verified by the S 2p signal (Figure 2b). This evidence suggests that either Pb−carboxylate or $PbSO_3$ serves as a sensitizing species having an (undesirably long-lived) ~420 ms time constant.

Table 1. Summary of the Correlation between Oxide Species and Photocurrent Time Constants Observed in Variously Treated PbS Nanocrystal Films

treatments	oxides	time constants
as synthesized	$PbSO_3$	
	Pb-carboxylate	
	$PbSO_4$	
butylamine	$PbSO_3$	∼60 ms
	Pb-carboxylate	∼300 ms
	$PbSO_4$	∼2 s
ethanethiol	$PbSO_3$	∼27 ms
ET + aging in ambient	$PbSO_3$	∼38 ms
	$PbSO_4$	∼3 s
Formic acid	$PbSO_3$	∼33 ms
	Pb-carboxylate	∼420 ms

In order to unmask which among the carboxylate/sulfite species is responsible for the ∼420 ms time constant, we sought to remove completely the oleate ligands. We sought a ligand, short enough to promote transport, and lacking carboxylate functionality. To make the replacement of the carboxylate-terminated ligand thermodynamically favorable, we posited that we would require an endgroup that would bind to the Pb more strongly than Pb−carboxylate. We selected ethanethiol for its short length and its thiol moiety expected to bind strongly with Pb. We treated the devices by dipping in 40% by volume ethanethiol in acetonitrile for approximately 5 min. We removed the device from solution, rinsed with acetonitrile, and dried.

From the absence of the Pb 4f peak at around 139.1 eV (Figure 2a), we conclude that oleate ligands were indeed entirely removed from the nanocrystal surface. Thiol treatment also removed polysulfites and lead sulfate from the nanocrystal surface leaving $PbSO_3$ as the sole oxidized species (Figure 2b). Transient photocurrent measurements showed that ethanethiol (ET) treated nanocrystal films exhibited a single transient component having a ∼27 ms time constant at room temperature (Figure 1).

We summarize in Table 1 the observed correlations between species and temporal components. We found that PbS nanocrystal films having lead sulfate ($PbSO_4$), lead sulfite ($PbSO_3$), and lead carboxylate manifested photocurrent decays having time constants ∼2 s, 300 ms, and ∼60 ms. PbS nanocrystals possessing lead carboxylate and $PbSO_3$ exhibited a photocurrent decay with time constants ∼420 and ∼33 ms. Thiol treated nanocrystals on which only lead sulfite was present exhibited a single photocurrent relaxation time constant of ∼27 ms. We confirmed the association between the sulfate and the 2 s time constant by aging a thiol-treated device in ambient for several hours: we found that a slow component emerged having the several-second time constant and found using XPS that significant growth of lead sulfate had taken place (see Supporting Information).

We sought to investigate in greater detail the energy level associated with the desired 27 ms trap state. In photoconductive photodetectors, photocurrent is given as

$$I_p = P\eta q\tau_c/h\nu\tau_t = P\eta q\tau_c \mu E/h\nu L$$

where P is the impinging optical power, η is the quantum efficiency (or absorbance), τ_c is the carrier lifetime, τ_t is the transit time, and E is the applied electric field across the
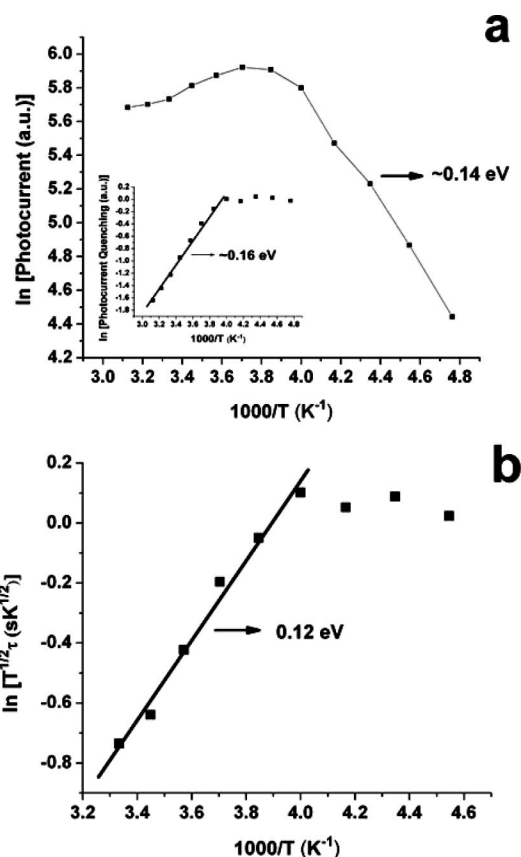

Figure 3. Photocurrent temperature spectroscopy results. (a) Photocurrent vs temperature and photocurrent quenching vs temperature (shown in inset) reveal a single sensitization center 0.16 eV below the conduction band. (b) Photocurrent temporal response as a function of temperature reveals an activation energy of the sensitizing center of 0.12 eV below the conduction band, in good agreement with the value extracted via photocurrent quenching.

device of length L. Photocurrent is thus proportional to mobility and carrier lifetime. In sensitized photoconductors, at low temperatures where all trap states act as sensitizing centers, i.e., the electron quasi-Fermi level lies between the trap state energies and conduction band edge, carrier lifetime is temperature insensitive.[12] Photocurrent then follows the mobility dependence on temperature which for nanocrystals solids has been reported to vary as:

$$\mu = \mu_0 e^{-E_a/kT}$$

where μ_0 is the temperature invariant mobility factor and E_a is the mobility activation energy.[13] With increasing temperature, the electron quasi-Fermi level drops followed by thermal depopulation (or desensitization) of the electron trap states. Carrier lifetime then becomes temperature dependent characterized by a thermal emission rate given by

$$\tau^{-1} = \sigma_n N_c \upsilon_{th} \exp(-\Delta E/kT)$$

where σ_n is the capture cross section of the trap, N_c is the density of states in conduction band, υ_{th} is the thermal velocity of the carriers, and ΔE is the energy depth of the trap measured relative to the conduction band edge. Photocurrent in this regime is determined by the two competing mechanisms of increasing mobility and decreasing lifetime with temperature, leading to photocurrent quenching.
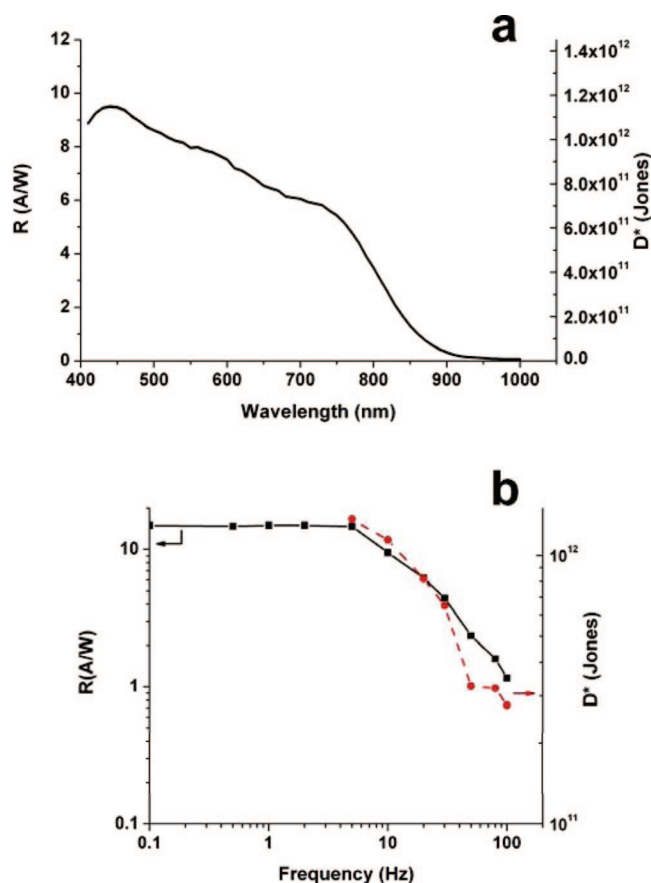
Figure 4. (a) Spectral responsivity and detectivity of the ethanethiol treated device considered a modulation frequency of 10 Hz. (b) Responsivity and specific detectivity as function of modulation frequency at 450 nm wavelength.

The method of experimental investigation and analysis is described in detail elsewhere.[9,12] Figure 3a shows the photocurrent as a function of temperature. At low temperatures, where the sensitizing centers are not thermally quenched, and therefore the devices are fully sensitized, responsivity increases with temperature following the mobility thermal activation of 0.14 eV similarly reported for such materials.[9,13] At elevated temperatures, photocurrent quenching takes place as a result of thermal deactivation of the sensitizing center. The slope of the quenching rate with temperature (inset of Figure 3a) yields an activation energy 0.16 eV from the conduction band. This agrees well with previous reports of the shallowest center in butylamine treated PbS nanocrystal photodetectors.[9] We ascertained the same activation energy using an independent method, investigating the dependence of the photocurrent transient on temperature.[12] This method provides a direct measurement of the trap state thermal emission rate. Using this method, therefore, we verified the sensitizing center's energy to be 0.12 eV below the conduction band, in reasonable agreement with the responsivity quenching results (Figure 3b).

We conclude with the results of full characterization of the thiol-treated device, focusing on its applicability to imaging applications requiring the combination of sensitivity and acceptable temporal response. The spectral responsivity is reported in Figure 3a.[14] Responsivity was measured at intensity levels of ~300 nW/cm^2 using a 642 nm LED. The device was biased to 10 V. We measured the noise current in the device[15] and plot in Figure 3a the detectivity, D^*.[6] Sensitivity is retained without compromise: D^* greater than 10^{12} Jones is obtained across the visible spectrum. Figure 3b also illustrates the device responsivity and detectivity as a function of modulation frequency. The absence of long-lived trap states is evident from the flat response of responsivity at frequencies below 5 Hz where the sensitizing centers associated with the ~400 ms and ~2 s time constants would determine the responsivity roll-off.[5,6]

We have shown herein the fine-tuning of macroscopically observed device performance via careful manipulation of the chemical species present on semiconductor nanoparticle surfaces. Specifically, we have transformed an unacceptably slow photoconductive photodetector into one that is sufficiently fast to respond to be suitable in imaging applications. By simultaneously reducing internanoparticle spacing, we achieved this improvement without compromising the highly desired photoconductive gain. More broadly, the work demonstrates the applied power of careful compositional control on the nanometer lengthscale.

Supporting Information Available: XPS analysis of variously treated PbS nanocrystal films. This material is available free of charge via the Internet at http://pubs.acs.org.

References

(1) Fossum, E. R. *IEEE Micro* **1998**, *18*, 8–15.
(2) Ettenberg, M. *Adv. Imaging* **2005**, *20*, 29–32.
(3) Kim, S.; Lim, Y. T.; Soltesz, E. G.; De Grand, A. M.; Lee, J.; Nakayama, A.; Parker, J. A.; Mihaljevic, T.; Laurence, R. G.; Dor, D. M.; Cohn, L. H.; Bawendi, M. G.; Frangioni, J. V. *Nat. Biotechnol.* **2004**, *22*, 93–97.
(4) Kymissis, I.; Akinwande, A. I.; Bulovic, V. *J. Display Technol.* **2005**, *1*, 289–294.
(5) Konstantatos, G.; Clifford, J.; Levina, L.; Sargent, E. H. *Nat. Photonics* **2007**, *1*, 531–534.
(6) Konstantatos, G.; Howard, I.; Fischer, A.; Hoogland, S.; Clifford, J.; Klem, E.; Levina, L.; Sargent, E. H. *Nature* **2006**, *442*, 180–183.
(7) Hegg, M.; Lin, L. Y. *Opt. Express* **2007**, *15*, 17163–17170.
(8) Oertel, D. C.; Bawendi, M. G.; Arango, A. C.; Bulovic, V. *Appl. Phys. Lett.* **2005**, *87*, 213505–213507.
(9) Konstantatos, G.; Sargent, E. H. *Appl. Phys. Lett.* **2007**, *91*, 173505–173507.
(10) PbS nanocrystals with an excitonic peak around 800 nm were synthesized by injection of 2.0 mmol of bis(trimethylsilyl sulfide) with 10 mL of octadecene into the reaction flask containing 4.0 mmol of lead oxide (0.9 g), 9.5 mmol of oleic acid (2.67 g), and 18.8 mmol of octadecene (4.73 g) at 70 °C. After the injection, the heater was turned off, but the heating mantel was not removed in order to let the reaction flask cool down slowly. When the temperature reached 30−35 °C the reaction was quenched with 40 mL of room temperature acetone. The synthesis was carried out under inert conditions using a Schlenk line. The final PbS oleate-capped nanocrystals were isolated from any remaining starting materials and side products purified by precipitating with acetone. The precipitate was then redissolved in toluene and precipitated again with acetone. The nanocrystals were then dried and transferred in inert atmosphere where they were redispersed in toluene for storage.
(11) Transient dark- and photoconductivity were measured using a 4155 Agilent semiconductor parameter analyzer.
(12) Espevik, S.; Wu, C.; Bube, R. H. *J. Appl. Phys.* **1971**, *42*, 3513.
(13) Ginger, D. S.; Greenham, N. C. *J. Appl. Phys.* **2000**, *87*, 1361.

(14) For spectral responsivity measurements a bias was applied to the sample connected in series with a 2 MΩ load resistor. Illumination was provide by a white light source (ScienceTech Inc. TH-2) dispersed by a Triax 320 monochromator and mechanically chopped at the frequency of interest. Optical filters were used to prevent grating overtones from illuminating the sample. The voltage across the load resistor was measured using a Stanford Research Systems SR830 lock-in amplifier. The intensity transmitted through the monochromator at each wavelength was precalibrated—and controlled via a variable attenuator—to be ~500 nW/cm^2. Photocurrent was then extracted by the ratio of the recorded voltage in the lock-in amplifier over the load resistor.

(15) Dark current noise in the photodetectors was measured using a Stanford Research SR830 lock-in amplifier. The devices were biased using alkaline batteries, and testing was done in an electrically shielded and optically sealed probe station on a floating table to minimize vibrational noise. The reported noise current, normalized to the measurement bandwidth, divided by the responsivity under the same measurement conditions yielded the noise equivalent power (NEP). The normalized detectivity D^* was obtained as a function of wavelength, applied bias, and center frequency by dividing the square root of the optically active area of the device by the NEP.

NL080373E